Multi-Molecule Field-Coupled Nanocomputing for the Implementation of a Neuron

Multi-Molecule Field-Coupled Nanocomputing for the Implementation of a Neuron

Giuliana Beretta, *Graduate Student Member, IEEE,* Yuri Ardesi, *Graduate Student Member, IEEE,* Mariagrazia Graziano, and Gianluca Piccinini

***Abstract*—In recent years, several alternatives have been proposed to face CMOS scaling problems. Among these, molecular Field-Coupled Nanocomputing is a paradigm that encodes information in the spatial charges distribution and promises to consume a minimal amount of power. In this technology, circuits have always been designed using the same molecule type, and logic functions are obtained through specific layouts. This work demonstrates that multi-molecule circuits, which use different kinds of molecules in the same layout, enhance the circuit features and set up a new way to conceive molecular Field-Coupled Nanocomputing. In particular, by inserting different molecules with specific characteristics into appropriate layout positions, it is possible to obtain an artificial neuron behavior using the Majority Voter layout.**

***Index Terms*—Molecular Field-Coupled Nanocomputing, Artificial neuron, Multi-molecule circuits, Modeling.**

I. Introduction

In recent years, CMOS scaling brought new challenges to face, mainly related to the extreme miniaturization of the channel length, which approached the atomic size [1]. Researchers proposed several solutions to overcome the limitations coming from the fabrication of nanometric transistors. Some of these solutions advance a way to treat information that does not use conduction, as domain wall logic exploiting magnetization or Field Coupled Nanocomputing (FCN) based on local field interactions [1]. The molecular FCN (mFCN) strongly emerges thanks to its two main intrinsic peculiarities: ultra-small devices and low power dissipation [2].

The mFCN paradigm encodes the information in the spatial charge distribution of molecules [3], [4]. Information propagates through the coupling of the electric fields generated by the charge distribution. Instead, according to the spatial arrangement of molecules, different logic gates are possible: it is the position of molecules that defines the logic gate rather than molecules type [5].

This paper proposes a way to model and analyze different molecules in the same circuit to enrich the standard position-based computation typical of this technology. We can reuse some well-known logic device layouts to implement more complex functionalities than their original ones. For this purpose, we demonstrate that by exploiting multiple types of molecules in the Majority Voter (MV) layout, the device behaves as an artificial neuron. The MV has already been addressed as a possible building block for neural computing within the general Quantum-dot Cellular Automata (QCA) paradigm [6]. Conversely, in our work, we propose a complete model from inputs to output. We also encode all the neuron features in the molecular characteristics, fulfilling our aim to demonstrate that multi-molecule circuits augment the mFCN paradigm functional capabilities. In addition, some works have already addressed how to deposit single molecules for biological applications technologically or to change the properties at the single-molecule level in a self-assembled monolayer, proposing techniques that may also help mFCN technology [7], [8].

The design of a neuron is well-suited for mFCN technology since molecules intrinsically have a non-linear behavior and the capability of adding up the effects of surrounding molecules [9]. These properties lead to a simple neuron structure at the architectural level, with a corresponding compact model. The presented model refers to a specific device aimed at a possible actual molecular implementation. Having a close model of a molecular device is advantageous in terms of computational resource requirements. Instead of evaluating all the interactions among molecules in a Self Consistent Field (SCF) loop, it is possible to predict the device output based on input configuration directly.

Overall, this work paves the way to a new perspective in designing complex mFCN devices and their modeling. So we present the design of a complete neuron with mFCN and the high-level functional model of the structure.

II. Background

The FCN paradigm finds a realization in different technologies, such as perpendicular Nano-Magnetic Logic (pNML) or molecular QCA [10], [11]. Using molecules, in particular, offers great advantages thanks to the possibility to work at room temperature, get very high-density circuits, exploit self-assembly fabrication techniques, consume a minimal amount of power, and work at a very high frequency [4], [12]–[16].

In mFCN, the position of the charge in molecules encodes the information. One of the most used molecules for this technology is the oxidized bis-ferrocene, shown in Fig. 1(a) [4], [9]. This molecule presents three functional groups, often called dots, in which the charge can locate according to the surrounding electric fields. As Fig. 1(b) and Fig. 1(c) show,

Manuscript sent May 28, 2021; Accepted 12 January, 2022

Giuliana Beretta (corresponding author, e-mail: giuliana.beretta@polito.it), Yuri Ardesi, and Gianluca Piccinini are with the Department of Electronics and Telecommunications, Politecnico di Torino, 10129 Turin, Italy.

Mariagrazia Graziano is with the Department of Applied Science and Technology, Politecnico di Torino, 10129 Turin, Italy.

DOI: 0000–0000/00$00.00

This article has been accepted for publication in IEEE Transactions on Nanotechnology. This is the author's version which has not been fully edited and content may change prior to final publication. Citation information: DOI 10.1109/TNANO.2022.3143720

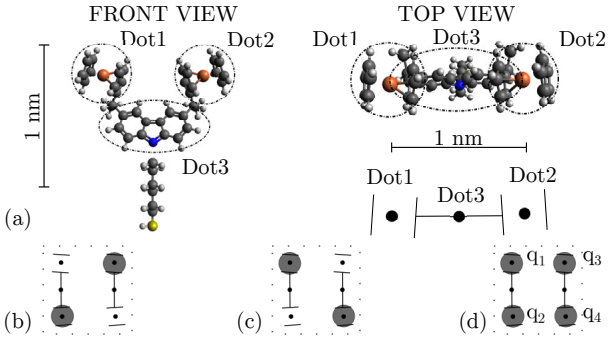

Fig. 1: Oxidized bis-ferrocene: (a) front and top views of its molecular structure, both with dots and dimensions highlighted, and a schematic representation of it, (b) grey circles represent the charge position in a unit cell encoding a logic '0', (c) grey circles represent the charge position in a unit cell encoding a logic '1', (d) the position of the i-th dot for the definition in equation (1).

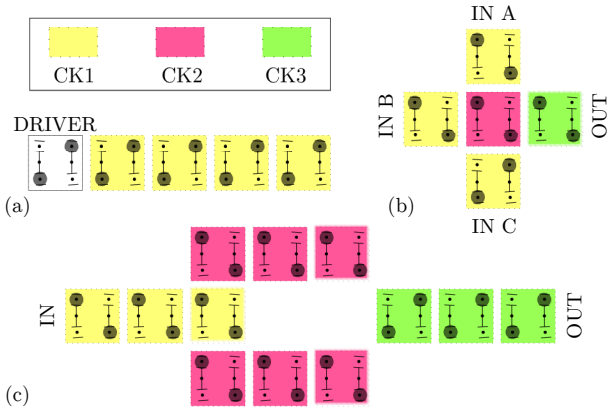

Fig. 2: Logic gates in mFCN technology: (a) a wire made of 4 unit cells propagating a logic '0', (b) a MV with logic inputs [1;1;0], (c) an inverter with a logic '1' as input.

two nearby molecules form a unit cell. Thanks to the repulsive Coulomb's force, the charge more likely localizes diagonally, occupying mostly one of the two logic dots (Dot 1 and Dot 2 of Fig. 1(a)). According to the occupied diagonal, it is possible to encode a logic '0' (Fig. 1(b)) or a logic '1' (Fig. 1(c)) [17]. Another useful quantity to define the logic state of a QCA cell is polarization, defined as

$$P = \frac{(q_1 + q_4) - (q_2 + q_3)}{q_1 + q_2 + q_3 + q_4} \quad (1)$$

where q_i is the charge of the i-th dot of the cell (Fig. 1(d)) [18].

As Fig. 2(a) shows, a mFCN wire able to propagate information is composed of a certain number of molecules placed in a row [19]. By fixing the charge distribution of the driver cell through an electric field, the other molecules will arrange their charge distribution according to Coulomb's force [20].

In this technology, logic gates are formed by placing molecules according to a particular layout. One fundamental logic gate, shown in Fig. 2(b), is the three-inputs MV, whose output equals the logic value on the majority of the inputs [5]. This gate is crucial since it also gives the two-input AND and the two-input OR gates when forcing one input value to logic '0' or logic '1', respectively. Fig. 2(c) shows the inverter layout instead. To invert a signal, the input wire should first split into two branches, hence duplicating the information. Then, the information onto those two arms recombines through a diagonal interaction [5]. Notice that all these circuits are made using the same molecule. In this work, we introduce a functional model to include the modifications brought in by the presence of more than one molecule in the circuit.

Besides this, we have to consider that the molecules spatial charge distribution generates an electric field all around. By introducing a clocking system, we help information propagate forward rather than backward [5]. The clock signal is a vertical electric field able to move the charge from the logic dots to a reset dot (Dot 3 of Fig. 1(a)), giving a NULL logic state. With the circuit divided into regions and providing out-of-phase clock signals, information propagates as in pipelined circuits. The colors in Fig. 2 depict different clocking regions: concerning their dimension, the literature offers practical alternative implementations that do not use single-cell zones [21], [22]. Nevertheless, this work focuses on the high-level closed-form functional model of mFCN circuits with more than one molecule type, employing the neuron case of study. We thus divide the layout into single-cell regions to easily identify and explain the different contributions to the whole functional model. In this way, the modeled effects can be efficiently extended to systems that use different clocking distributions.

III. Methodology

The methodology we use in this work is called MoSQuiTo (Molecular Simulator Quantum-dot cellular automata Torino), which consists of three steps [23]: ab initio simulations, electrostatic parameters extraction, and quasi-physical simulations.

The first step of the MoSQuiTo methodology consists of ab initio simulations to analyze the molecules of interest stimulated with different electric fields. At this point, the molecule is described by a set of atomic charges derived from ab initio calculations by fitting the electrostatic potentials.

In the MoSQuiTo second step, all the collected data are processed to extract high-level parameters describing the electrostatic behavior of molecules: we mainly use the Aggregated Charge (AC) and the input voltage (V_{in}) of a molecule [9], [23]. The AC is the sum of all the atomic charges belonging to the same dot. The input voltage of a molecule is the equivalent voltage between the two logic dots generated by the surrounding electric fields (Fig. 3). The relation between these two figures of merit gives the Voltage-Aggregated Charge Transcharacteristic (VACT), which describes the behavior of the ACs of a single molecule varying its input voltage [9]. Fig. 3 shows the VACT of the bis-ferrocene when the clock signal enables the molecule, and two regions can be recognized: in the central one, the curves of the logic dots AC are linear, whereas externally, the logic dots AC saturates [9]. We define as V_{SAT} the absolute value of the voltage for which the molecule enters the saturation region (V_{SAT} = 0.5 V for the bis-ferrocene). Generally, molecules VACT shows a linear trend

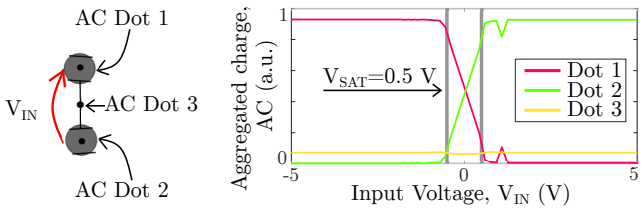

Fig. 3: Voltage-Aggregated Charge Transcharacteristic (VACT) of the bis-ferrocene and a schematic representation of the aggregated charges and the input voltage of a molecule [23].

for logic dots in a region more or less extended depending on the specific molecule [24]. Moreover, even when molecules ACs do not saturate, the functionality of the systems is not affected.

The last step of the MoSQuiTo methodology consists of circuit analyses using the figures of merit extracted at the previous point. The VACTs are used to derive the circuit behavior employing a Self Consistent ElectRostatic Potential Algorithm (SCERPA) [5], [25]. SCERPA is an algorithm that permits the quasi-physical simulations of mFCN circuits, using the electrostatic parameters defined through MoSQuiTo. By employing an iterative procedure (SCF loop), it calculates the AC values of each molecule composing the circuit.

In this work, we take the bis-ferrocene VACT as a reference, and we tune it to understand which effects the electrostatic characteristics produce at the system level. Nevertheless, the real molecules presenting those characteristics are not necessarily based on bis-ferrocene structure: they can be completely different. The SCERPA algorithm provides sufficient flexibility to consider different molecules in the same circuit [25]. By giving SCERPA some ad-hoc defined VACT, it is possible to relate the molecules electrostatic with the specific circuit behavior. This procedure allows us to study complex systems, such as artificial neurons, from a functional point of view without necessarily having all the characteristics of the actual molecules. In this way, instead of analyzing the high-level circuits built with specific molecules, we have been able to design a circuit, fixing the properties that molecules should have to accomplish a particular task within the layout.

This approach goes in the direction of providing chemists valuable indications on how the molecule should be, thus acting as a guide for a possible prototype of mFCN. In the last decade, chemists have already synthesized ad-hoc molecules for molecular electronics [26]. In the future, these studies can extend to the synthesis or functionalization of molecules suitable for a specific task in mFCN.

IV. Design

The circuit we want to design is an artificial neuron, starting from the MV layout. As shown in Fig. 4, a neuron is generally a system that receives a certain number N of inputs x_i. Each input is associated with a weight w_i used to increase or diminish the effect of that particular signal. A sum operation combines those weighted inputs as follows

$$s = \sum_{i=1}^{N} w_i \cdot x_i \tag{2}$$

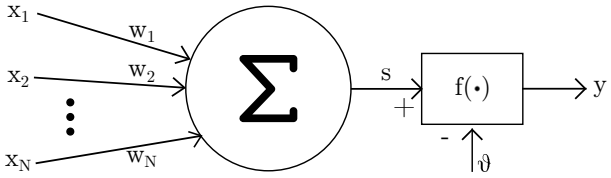

Fig. 4: Schematic representation of an artificial neuron.

The total contribution of the inputs s is then used to evaluate the activation of the neuron, through an activation function $f(s)$, which is a specific non-linear function [27]. Finally, the output of the neuron y is calculated, eventually comparing the value with a threshold ϑ, as expressed below

$$y = f(s - \vartheta) \tag{3}$$

To design the artificial neuron, we analyze each part of it separately. First, we discuss the choice to use a MV as an underlying structure, and we define the quantity we associate with each signal. We then discuss how we encode weights, implement the activation function, propagate output, and include a threshold mechanism. Finally, we propose a possible structure to add a fourth input, discussing how the behavior changes and, consequently, how to modify the model. Since we are interested in modeling the interactions between different molecules in a device, we use simple clocking schemes for both the three-inputs and the four-inputs layouts: this allows us to focus on the interactions that affect the high-level parametrization of the device.

A. Addition and variables definition

The most simple mechanism to perform the addition is the superposition effect of electric fields between nearby cells. To demonstrate it, we consider the structure of Fig. 5, where two input cells (up and down) propagate their information toward the central cell. In this structure, considering the ideal input configurations, there are four possible situations. As shown in Fig. 5(a), when inputs have both a polarization equal to $P_{IN1} = P_{IN2} = -1$, their addition on the central cell would be $P_{IN1} + P_{IN2} = -2$, which traduces to $P_{OUT} = -1$ for equation (1). A similar situation occurs in Fig. 5(b) when both inputs have a polarization $P_{IN1} = P_{IN2} = +1$. In the case

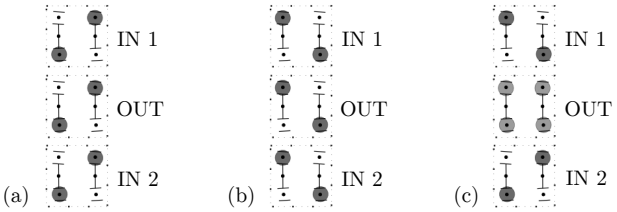

Fig. 5: Superposition effect in mFCN: (a) inputs have both $P_{IN1} = P_{IN2} = -1$, their addition would be $P_{IN1} + P_{IN2} = -2$, so the output polarization is $P_{OUT} = -1$, (b) inputs have both $P_{IN1} = P_{IN2} = 1$, their addition would be $P_{IN1} + P_{IN2} = 2$, so the output polarization is $P_{OUT} = 1$, (c) inputs are $P_{IN1} = 1$ and $P_{IN2} = -1$, so $P_{OUT} = 0$ (if inputs exchange their values, the output is the same).

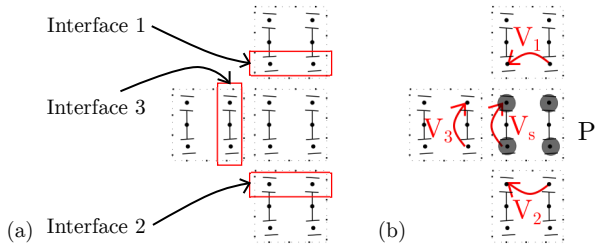

Fig. 6: Definition of the quantities associating the general signals in an artificial neuron implemented through a MV: (a) numbering of the interfaces, (b) input signals V_i with i = [1:3], sum signal V_s and the polarization of the cell with the grey circles is the output signal P.

of Fig. 5(c), inputs have opposite polarization, so the charge equally distributes on the dots constituting the central cell, leading to a polarization $P_{OUT} = 0$.

The same mechanism occurs in the MV, so we use it as an underlying structure to perform the addition. We then have to define the physical quantities associated with the general signals (x_i, s, and y) of equations (2) and (3). Fig. 6(a) shows the enumeration of the inputs used hereafter and also the dots couples which constitute the interfaces near the three input faces of the MV central cell. We then define the input signals (x_i) as the input voltages on the interface V_i, as shown in Fig. 6(b), where i = [1:3]. The fact that V_1 and V_2 are defined across two different molecules does not affect the behavior: in the case in which those two molecules have the same VACT, the interface behaves as if a single molecule with the same VACT is placed horizontally inside the interface rectangles of Fig. 6(a).

The input voltage on the first molecule of the central cell V_s considers all the input contributions, so we associate it with the signal s. The polarization P of the MV central cell is the neuron output signal y (Fig. 6). Neglecting the threshold θ, for now, thanks to the definitions just explained, equations (2) and (3) can be rewritten as

$$P = f(V_s) = f\left(\sum_{i=1}^{N} w_i \cdot V_i\right) \tag{4}$$

where $N = 3$, the function f is a non-linear function that links V_s and P, and w_i are the weights that link V_i and V_s.

B. Weights

Equation (4) highlights that weights are encoded in the relation between the interfaces input voltages V_i and the sum voltage V_s. Interface molecule characteristics affect that relation, since varying their VACT slope, interfaces global effect on V_s varies accordingly. If we refer to the ad-hoc defined VACTs of Fig. 7, by fixing the molecule input voltage V_{IN}, the difference between the AC on Dot1 and Dot2 increases when the VACT slope increases as well. Consequently, the effect of the interfaces on the sum voltage V_s grows with the VACT slope of the interfaces.

To ensure a correct addition, V_i and V_s must follow a linear relation, that is, the V_{SAT} of interface molecules must be outside the range of possible voltages occurring in a circuit: we thus have a lower bound for interfaces V_{SAT}. To find the maximum voltage present in a circuit and the minimum VSA for interface molecules, V_{SAT} for interface molecules, we simulate a classical MV with inputs and output connected to wires composed of 8 cells. In this way, we reproduce a working condition in which several cells are active. Analyzing those simulations, we find that the input voltage of all molecules always belongs to the range [-1;+1] V. Thus the minimum possible saturation voltage to ensure linearity is $V_{SAT} = 1$ V. The five ad-hoc designed VACTs of Fig. 7 comply with the condition on minimum V_{SAT}, and so we use them hereafter as interface molecule VACTs.

TABLE I: Weights calculated for the three interfaces corresponding to five molecules with a different V_{SAT}.

V_{SAT} (V)	w_1 (-)	w_2 (-)	w_3 (-)
1.0	0.3353	0.3353	0.4436
1.5	0.2287	0.2287	0.3020
2.0	0.1741	0.1741	0.2299
2.5	0.1406	0.1406	0.1856
3.0	0.1179	0.1179	0.1556

The constraint on V_{SAT} fixes also the upper bound for weights. TABLE I lists the weights corresponding to the five VACTs represented in Fig. 7. Those values, rounded to the fourth decimal position to correctly see the error propagation hereafter, are calculated through equation (5)

$$w_i = -\frac{V_{s_i}}{V_i} \quad \text{for } i = 1, 2, 3 \tag{5}$$

where V_{s_i} indicates the input voltage of the first molecule of the central cell of the MV due only to the effect of the i-th input. In order to consider just one input at a time, the input voltage on the other two inputs has been fixed to zero, so none of the two logic states is favored. The minus sign derives from the inversion mechanism present to one molecule and the next.

Data in TABLE I demonstrate that the smaller V_{SAT} (higher slope), the higher the weight. Moreover, we see that interfaces have not all the same effect. Indeed, interface 3 affects the first molecule of the MV central cell more than interfaces 1 and 2, which are instead equivalent. This difference comes from the distance between interface 3 and the first molecule

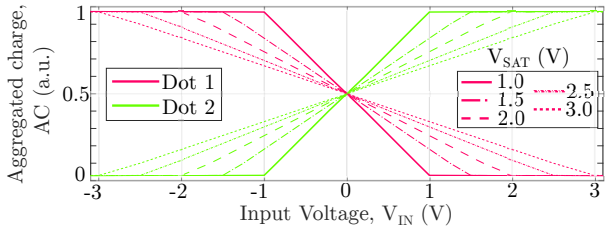

Fig. 7: Ad-hoc defined VACTs of five molecules with different V_{SAT}, so with different weights (different slope). Each VACT is composed of a dark pink line for dot 1 and a light green line for dot 2: the line style associates the two curves for logic dots of each molecule type.

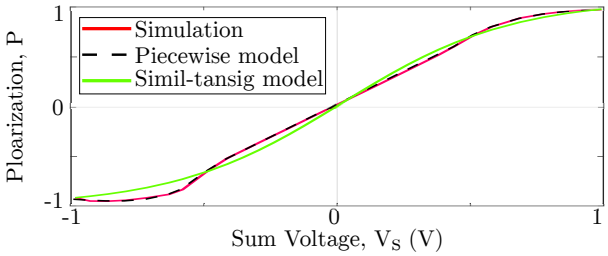

Fig. 8: Polarization P of a cell composed by two bis-ferrocenes with respect to the input voltage V_s on the first molecule of the same cell: comparison between the simulation done with SCERPA, a piecewise model, and a simil-tansig model (both models are the result of a fitting procedure).

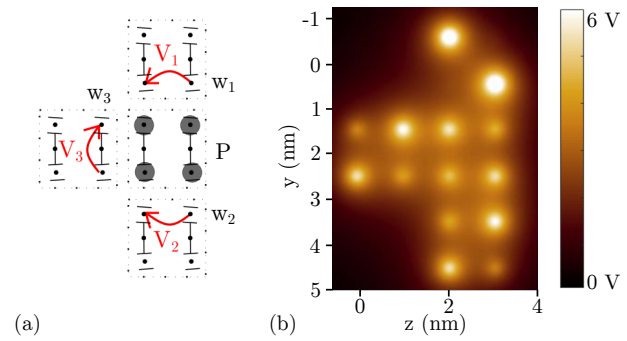

Fig. 9: Example: (a) layout of the example and variables of interest, (b) electric potential distribution evaluated at 0.2 nm above the active dot plane (result produced by SCERPA).

of the MV central cell, which is smaller than those of the other two interfaces.

C. Activation Function

Activation functions are non-linear function that defines the output of a neuron [27]. When using molecules, non-linearity can be easily found in VACTs, as already seen in Fig. 3. As expressed by equation (4), we need a non-linear function that links the sum voltage V_s and the polarization P of the MV central cell. Moreover, the range of voltages in a circuit is [-1;1] V, and bis-ferrocene V_{SAT} is inside that range, so we can use it directly to compose the central cell of the MV. Fig. 8 shows the activation function obtained by simulating a MV in which two bis-ferrocenes compose the central cell.

The dashed curve in Fig. 8 represents the piecewise model of the activation function simulated for our neuron, obtained through a fitting procedure which gives the following formula

$$\begin{cases} a_1 \cdot e^{b_1 \cdot V_s} + c_1 \cdot e^{d_1 \cdot V_s} & V_s \leq -0.48 \\ p_1 \cdot V_s + p_2 & -0.48 < V_s < 0.48 \\ a_2 \cdot e^{b_2 \cdot V_s} + c_2 \cdot e^{d_2 \cdot V_s} & V_s \geq -0.48 \end{cases} \quad (6)$$

where a_i, b_i, c_i, d_i and p_i (i = 1,2) are the fitting parameters.

To get a simpler model than equation (6), we consider typically used activation functions. The best approximation of the curve obtained from the SCERPA simulation is given by the tan-sigmoid function (tansig), which is described by the following equation [27]

$$y = \text{tansig}(x) = \frac{2}{1 + e^{-2x}} - 1 \quad (7)$$

We decide to refine the tansig expression of equation (7), through a fitting procedure, to reduce the error of the approximation. The best obtainable fit of the simulated activation function is the simil-tansig curve in Fig. 8, which is described by the equation below

$$P = f(V_s) = \frac{a}{b + e^{-c \cdot V_s}} - 1 \quad (8)$$

where $a = 1.959$, $b = 0.945$, $c = 3.166$ V^{-1} are the values of the parameters extracted from the fitting procedure.

At this point, we can present an example to confirm the validity of the proposed design. Fig. 9(a) shows the considered structure, where interface 1 is a cell composed by two molecules with $V_{SAT} = 1$ V, whereas interfaces 2 and 3 are cells composed by two molecules each with $V_{SAT} = 3$ V. The input voltages and the weights for each interface are:

- interface 1: $V_1 = +1$ V and $w_1 = 0.3353$;
- interface 2: $V_2 = -1$ V and $w_2 = 0.1179$;
- interface 3: $V_3 = -1$ V and $w_3 = 0.1179$.

Following equation (8), the polarization of the central cell of the MV is $P = 0.1694$. From the simulation in SCERPA of the circuit we extract a polarization $P = 0.1636$. Fig. 9(b) shows the electric potential distribution evaluated at 0.2 nm above the active dot plane of the considered layout, where the light circles indicate the presence of a positive charge. From Fig. 9(b), we can see that interface 1 encodes an opposite logic value to those of the other two interfaces (as the input voltages say), visible from the bigger spot on different diagonals. The signal strength of interface 1 is higher than interfaces 2 and 3 (as the weights say): on the graph, it is represented by the more distributed charge configuration of inputs 2 and 3. The central cell presents a charge on all its four dots, which means its value is far from the ideal ± 1 (as confirmed by the calculated result). Moreover, it is also possible to infer the polarization sign: since the charge on the central cell is more located on the same diagonal of interface 1, the polarization would be positive, as confirmed from the mathematical result.

D. Output propagation

Once calculated the weighted sum, the neuron needs to propagate the result. Generally, all the molecules in a wire should stay in the saturation region to propagate information correctly. Also, the wire should be composed of a minimum number of molecules for each clock region that help strengthen information encoded in the wire [28].

In our scenario, the output wire driver molecules are those in the MV central cell, which can be out of saturation. By considering, for instance, the situation of the example in section IV-C, the driver molecules for the output wire encode a polarization P = 0.1636, which is too weak to drive a wire. To verify this, consider the layout of Fig. 10(a), in which there is a wire composed of 16 bis-ferrocene molecules, driven by two other bis-ferrocene molecules that encode the polarization P = 0.1636 as the MV central cell simulated in

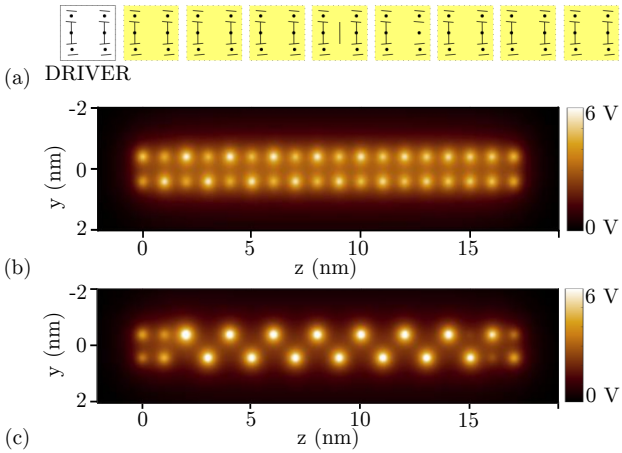

Fig. 10: Example of information propagation when the output wire is driven by two bis-ferrocene molecules encoding a polarization $P = 0.1636$: (a) layout considered for the example, (b) electric potential distribution, evaluated at 0.2 nm above the active dot plane, of the simulation done with SCERPA, (c) with a saturator just after the driver cell.

the example of section IV-C. Fig. 10(b) shows the electric potential distribution, evaluated at 0.2 nm above the active dot plane, of the simulation done with SCERPA: the information is lost in the second half of the wire as was presumed.

Inserting a molecule with a tiny V_{SAT} (charge saturator) at the beginning of the output wire solves the problem just exposed. By considering Fig. 10(a) again, and substituting the bis-ferrocene molecule after the drivers with a molecule with $V_{SAT} = 0.1$ V, the charge profile of the output wire changes completely, as confirmed by the simulation done with SCERPA and shown in Fig. 10(c). In this case, information propagates through the whole wire, but the polarization at the end of the wire is different from the information encoded by the driver cell. To consider the saturation effect in the model, the equivalent function seen from the outside of the neuron must tend to the sign function

$$P_{out} = \begin{cases} -1 & P < 0 \\ 0 & P = 0 \\ 1 & P > 0 \end{cases} \tag{9}$$

where P_{out} is the polarization of the first cell of the output wire, in which a saturator molecule is present.

E. Threshold mechanism

One feature that neurons can present is comparing the result of the weighted sum with a threshold, which means to have the activation function shifted toward left or right depending on the sign of the threshold.

To get a shifted activation function, we have to use molecules that present a shift in their VACT instead of bis-ferrocene in the MV central cell, as schematically represented in Fig. 11(a). Fig. 11(b) shows two possible shifted VACT, where even with no voltage applied, there is more charge localized on one of the two logic dots, depending on the shift

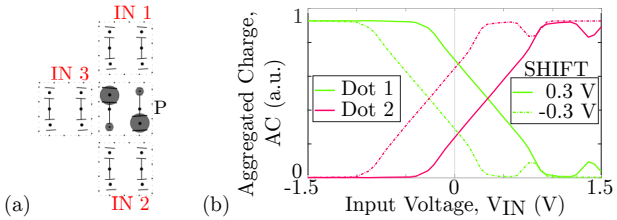

Fig. 11: The threshold mechanism in mFCN: (a) equivalent representation of molecules with shifted VACTs in the MV central cell, (b) example of VACT shifted of 0.3 V and of -0.3 V.

sign. To form a complete cell, we have to ensure that one of the two diagonals is more charge attractive. If the first molecule of the cell more likely localizes charge on Dot 1, the second molecule should have the same behavior with Dot 2 instead, which means that two molecules with opposite shifts in their VACT compose the cell.

Using different couples of shifted VACTs and simulating the system for the whole range of possible sum voltages, we calculate the polarization P for each V_s. Through the interpolation of the values obtained, we extract the activation function for different thresholds. Fig. 12 shows the simulated activation function for six different thresholds, together with the activation function obtained when bis-ferrocene molecules are placed at the center of the MV. The VACTs used to obtain those activation functions equal those represented in Fig. 11(b) unless the shift value. The shift sign of the activation function is the same as the second molecule of the MV central cell. For example, if we want a shift of the activation function equal to +0.3 V, then the first molecule of the central cell must have a VACT shifted of -0.3 V, whereas the second molecule must have a shift equal to +0.3 V.

F. Extension to more than three inputs

Since the structure presented so far has three inputs, we decided to extend the MV basic structure to have the possibility to add a fourth input. Fig. 13(a) shows the proposed layout, in which the output node is now expanded to three cells.

We first try to reuse the model presented in equation (8), by simply adding a fourth contribution to the calculation of the sum voltage V_s and recalculating the weights. TABLE II lists the weights for the same saturation voltages used in the previous sections. Even adapting the weights, the result of

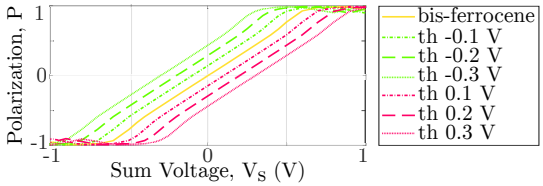

Fig. 12: Activation function comparison for different thresholds with the reference case in which two bis-ferrocene molecules are used in the central cell of the MV. The curves are interpolations of the result produced by SCERPA.

TABLE II: Weights calculated for the four interfaces corresponding to five molecules with a different V_{SAT}.

V_{SAT} (V)	w_1 (-)	w_2 (-)	w_3 (-)	w_4 (-)
1.0	0.3706	0.1882	0.1879	0.3720
1.5	0.2438	0.1245	0.1246	0.2426
2.0	0.1819	0.0921	0.0933	0.1822
2.5	0.1456	0.0732	0.0748	0.1467
3.0	0.1217	0.0613	0.0625	0.1228

the model is far from the outcome of the simulations. By considering, as an example, the following inputs

- interface 1: $V_1 = +1$ V and $w_1 = 0.3706$,
- interface 2: $V_2 = +1$ V and $w_2 = 0.1882$,
- interface 3: $V_3 = -1$ V and $w_3 = 0.0625$,
- interface 4: $V_4 = -1$ V and $w_4 = 0.1228$,

the result simulated with SCERPA is $P = 0.2880$ (Fig. 13(b)), whereas the prediction of the model is $P = 0.5648$.

The error in the output prediction comes from the layout differences that transform the high-level model. The weighted sum is now divided into two partial additions that can be computed in parallel, as highlighted in Fig. 14(a). Referring to Fig. 14(a), the division into two partial additions, called $P_{(a)_{TOP}}$ and $P_{(a)_{BOTTOM}}$, can be expressed as follows

$$\begin{aligned} P_{(a)_{TOP}} &= f(w_1 \cdot V_1 + w_2 \cdot V_2) \\ P_{(a)_{BOTTOM}} &= f(w_3 \cdot V_3 + w_4 \cdot V_4) \end{aligned} \tag{10}$$

where the function f is the same as equation (8) and the weights equals those in TABLE I, since the two partials additions are performed on a structure attributable to a MV. In addition, we have to include in the model others interaction between molecules, as the angular one between inputs 2 (and 3) and the cell in phase 2 (Fig. 14(b)), and the information reinforcement when both phase 1 and 2 are active (Fig. 14(c)).

Fig. 14(b) shows the angular interactions, which model the direct influence of the charge distribution of inputs 2 and 3 on the output cell: equation (11) describes each of these two interactions with the sum of two terms. The first term, related to the charge, depends on the interface molecule type and input voltage. The other term is related to the mutual position of the involved cells, which is therefore constant. The subscript

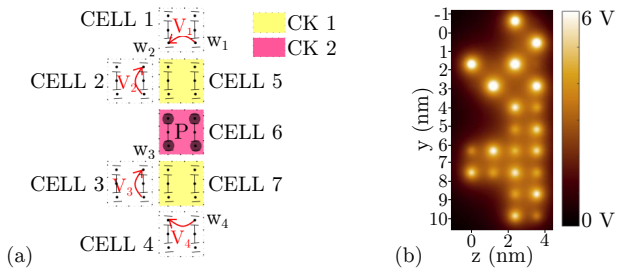

Fig. 13: Molecular FCN implementation of an artificial neuron with four inputs: (a) proposed layout, (b) electric potential distribution, evaluated at 0.2 nm above the active dot plane, of the simulation done with SCERPA of the proposed example.

TABLE III: Parameters present in the model for the angular interaction defined in equation (11) corresponding to five molecules with a different V_{SAT}.

V_{SAT} (V)	m_2 (V^{-1})	p_2 (-)	m_3 (V^{-1})	p_3 (-)
1.0	-0.1102	-0.2262	-0.1132	0.2188
1.5	-0.0746	-0.2262	-0.0779	0.2188
2.0	-0.0558	-0.2262	-0.0589	0.2188
2.5	-0.0441	-0.2262	-0.0466	0.2188
3.0	-0.0369	-0.2262	-0.0391	0.2188

numbers in equation (11) are associated with the considered input, referring to Fig. 14(b).

$$P_{(b)} = (m_2 \cdot V_2 + p_2) + (m_3 \cdot V_3 + p_3) \tag{11}$$

To obtain the parameters in equation (11), we simulate a system with only cell 2 (or cell 3) and cell 6. Then, repeating the simulation with different interfaces, we find the values listed in TABLE III. Data confirm what is explained so far, since m_2 and m_3 depend on the molecule VACT, whereas p_2 and p_3 are constant and, consequently, independent of the molecule characteristics. Moreover, p_2 and p_3 have a similar absolute value and an opposite sign, so globally, they cancel each other out.

Fig. 14(c) shows the mutual reinforcement of the charge distribution of cells 5 to 7, which is the second effect to consider. This interaction is modeled through a multiplicative coefficient that affects the partial sums expressed in equation (10). The coefficients are obtained simulating a structure in which only cells 5 to 7 and cell 1 (or cell 4) are present. For downward propagation, the ratio between the polarization of cells 5 and 6 gives the coefficient $m_{1,2} = 0.6846$, whereas, for upward propagation, the ratio between the polarization of cells 7 and 6 gives the coefficient $m_{3,4} = 0.5966$. By merging the three new interactions, the complete model becomes

$$\begin{aligned} P = m_{1,2} \cdot f(w_1 \cdot V_1 + w_2 \cdot V_2) + m_2 \cdot V_2 + p_2 + \\ m_{3,4} \cdot f(w_3 \cdot V_3 + w_4 \cdot V_4) + m_3 \cdot V_3 + p_3 \end{aligned} \tag{12}$$

By considering again the example at the beginning of this section, the result simulated with SCERPA is $P = 0.2880$ (Fig. 13(b)), whereas the prediction of the model expressed by equation (12) is $P = 0.2937$. As confirmed by the example, considering all the effects introduced with the layout increase the accuracy of the high-level model.

V. Conclusion

This work investigates the possibility of using more than one type of molecule in molecular FCN circuits to demonstrate that it is possible to change the functionality of a circuit. In particular, we concentrate on the majority voter layout, and we prove that by inserting different molecule types in it, the majority voter behaves like an artificial neuron. That means that without changing the layout of a circuit, we can modify its working principle by adequately choosing the electrostatic characteristics of the involved molecules.

We demonstrate and model the effects of the molecules' electrostatics onto the high-level functioning of the considered circuit, aiming to map molecules behavior with specific

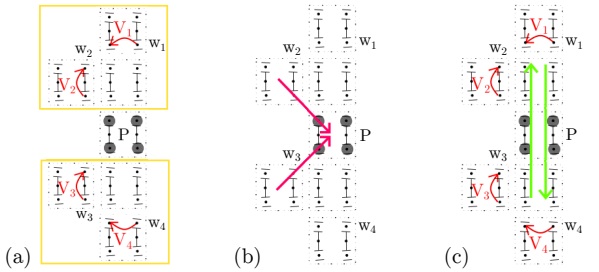

Fig. 14: Schematic representation of the effects to consider in the model for the artificial neuron with four inputs: (a) partial weighted sum, (b) angular direct interaction between lateral inputs and output, (c) propagation and back-propagation onto the three cells of the output node.

mechanisms inside the neuron, as the weights implementation or the threshold mechanism. We principally work with the relation between the molecular charge trend under different applied electric fields. That choice allows us also to generalize the analysis to hypothetical molecule characteristics. Instead of designing circuits using specific molecules and seeing if and how all work, we can define the requirements molecules should meet and eventually cooperate with chemists to design them.

Another key aspect of this work deals with the definition of high-level closed-form circuits models that would permit to avoid simulating them through self-consistent procedures, increasing the computational cost. Thanks to closed-form models of fundamental devices, we can study variously sized circuits composed of several parts with a reduced and controlled computational cost.

REFERENCES

[1] IEEE, "The international roadmap for devices and systems (irds)," 2020.

[2] C. S. Lent and G. L. Snider, *The Development of Quantum-Dot Cellular Automata*, pp. 3–20. Berlin, Heidelberg: Springer Berlin Heidelberg, 2014.

[3] C. S. Lent, B. Isaksen, and M. Lieberman, "Molecular quantum-dot cellular automata," *Journal of the American Chemical Society*, vol. 125, no. 4, pp. 1056–1063, 2003. PMID: 12537505.

[4] V. Arima, M. Iurlo, L. Zoli, S. Kumar, M. Piacenza, F. Della Sala, F. Matino, G. Maruccio, R. Rinaldi, F. Paolucci, M. Marcaccio, P. G. Cozzi, and A. P. Bramanti, "Toward quantum-dot cellular automata units: thiolated-carbazole linked bisferrocenes," *Nanoscale*, vol. 4, pp. 813–823, 2012.

[5] Y. Ardesi, G. Turvani, M. Graziano, and G. Piccinini, "Scerpa simulation of clocked molecular field-coupling nanocomputing," *IEEE Transactions on Very Large Scale Integration (VLSI) Systems*, pp. 1–10, 2021.

[6] E. P. Blair and S. Koziol, "Neuromorphic computation using quantum-dot cellular automata," in *2017 IEEE International Conference on Rebooting Computing (ICRC)*, pp. 1–4, 2017.

[7] S. K. Kufer, E. M. Puchner, H. Gumpp, T. Liedl, and H. E. Gaub, "Single-molecule cut-and-paste surface assembly," *Science*, vol. 319, no. 5863, pp. 594–596, 2008.

[8] K. Cui, K. S. Mali, D. Wu, X. Feng, K. Müllen, M. Walter, S. De Feyter, and S. F. Mertens, "Ambient bistable single dipole switching in a molecular monolayer," *Angewandte Chemie*, vol. 132, no. 33, pp. 14153–14157, 2020.

[9] Y. Ardesi, A. Pulimeno, M. Graziano, F. Riente, and G. Piccinini, "Effectiveness of molecules for quantum cellular automata as computing devices," *Journal of Low Power Electronics and Applications*, vol. 8, no. 3, 2018.

[10] U. Garlando, F. Riente, G. Turvani, A. Ferrara, G. Santoro, M. Vacca, and M. Graziano, "Architectural exploration of perpendicular nano magnetic logic based circuits," *Integration*, vol. 63, pp. 275 – 282, 2018.

[11] C. S. Lent, B. Isaksen, and M. Lieberman, "Molecular quantum-dot cellular automata," *Journal of the American Chemical Society*, vol. 125, no. 4, pp. 1056–1063, 2003. PMID: 12537505.

[12] C. S. Lent, "Bypassing the transistor paradigm," *Science*, vol. 288, no. 5471, pp. 1597–1599, 2000.

[13] Y. Ardesi, A. Gaeta, G. Beretta, G. Piccinini, and M. Graziano, "Ab initio molecular dynamics simulations of field-coupled nanocomputing molecules," *Journal of Integrated Circuits and Systems*, vol. 16, no. 1, pp. 1–8, 2021.

[14] J. Y. Cheng, F. Zhang, V. P. Chuang, A. M. Mayes, and C. A. Ross, "Self-assembled one-dimensional nanostructure arrays," *Nano Letters*, vol. 6, no. 9, pp. 2099–2103, 2006. PMID: 16968033.

[15] S. Srivastava, S. Sarkar, and S. Bhanja, "Estimation of upper bound of power dissipation in qca circuits," *IEEE Transactions on Nanotechnology*, vol. 8, no. 1, pp. 116–127, 2009.

[16] E. Blair, E. Yost, and C. Lent, "Power dissipation in clocking wires for clocked molecular quantum-dot cellular automata," *Journal of Computational Electronics*, vol. 9, p. 49–55, 2010.

[17] A. Pulimeno, M. Graziano, and G. Piccinini, "Molecule interaction for qca computation," in *2012 12th IEEE International Conference on Nanotechnology (IEEE-NANO)*, pp. 1–5, 2012.

[18] Y. Lu and C. S. Lent, "A metric for characterizing the bistability of molecular quantum-dot cellular automata," *Nanotechnology*, vol. 19, p. 155703, mar 2008.

[19] M. Graziano, R. Wang, M. R. Roch, Y. Ardesi, F. Riente, and G. Piccinini, "Characterisation of a bis-ferrocene molecular qca wire on a non-ideal gold surface," Jan 2019.

[20] A. Pulimeno, M. Graziano, D. Demarchi, and G. Piccinini, "Towards a molecular qca wire: simulation of write-in and read-out systems," *Solid-State Electronics*, vol. 77, pp. 101–107, 2012. Special Issue of IEEE INEC 2011(IEEE International Nano Electronics Conference).

[21] E. Blair and C. Lent, "Clock topologies for molecular quantum-dot cellular automata," *Journal of Low Power Electronics and Applications*, vol. 8, no. 3, 2018.

[22] J. Retallick and K. Walus, "Low-energy eigenspectrum decomposition (leed) of quantum-dot cellular automata networks," *IEEE Transactions on Nanotechnology*, vol. 20, pp. 104–112, 2021.

[23] A. Pulimeno, M. Graziano, A. Antidormi, R. Wang, A. Zahir, and G. Piccinini, *Understanding a Bisferrocene Molecular QCA Wire*, pp. 307–338. Berlin, Heidelberg: Springer Berlin Heidelberg, 2014.

[24] P. W. Atkins and J. De Paula, *Physical Chemistry*. Oxford University Press, 8 ed., 2006.

[25] Y. Ardesi, R. Wang, G. Turvani, G. Piccinini, and M. Graziano, "Scerpa: A self-consistent algorithm for the evaluation of the information propagation in molecular field-coupled nanocomputing," *IEEE Transactions on Computer-Aided Design of Integrated Circuits and Systems*, vol. 39, no. 10, pp. 2749–2760, 2020.

[26] J. M. Tour, "Molecular electronics. synthesis and testing of components," *Accounts of Chemical Research*, vol. 33, no. 11, pp. 791–804, 2000. PMID: 11087316.

[27] S. Sharma, S. Sharma, and A. Athaiya, "Activation functions in neural networks," *International Journal of Engineering Applied Sciences and Technology*, vol. 4, no. 12, pp. 310–316, 2020.

[28] Y. Ardesi, L. Gnoli, M. Graziano, and G. Piccinini, "Bistable propagation of monostable molecules in molecular field-coupled nanocomputing," in *2019 15th Conference on Ph.D Research in Microelectronics and Electronics (PRIME)*, pp. 225–228, 2019.